International Journal of GEOMATE, Nov., 2025 Vol.29, Issue 135, pp.80-87
ISSN: 2186-2982 (P), 2186-2990 (O), Japan, DOI: https://doi.org/10.21660/2025.135.5106
Geotechnique, Construction Materials and Environment

RELIABILITY-BASED EVALUATION OF FINE GRAIN EFFECTS ON LIQUEFACTION RESISTANCE

*Sumiyati Gunawan and Vienti Hadsari

Departement of Civil Engineering, Atma Jaya Yogyakarta University, Indonesia

*Corresponding Author, Received: 30 June 2025, Revised: 03 Sep. 2025, Accepted: 11 Sep. 2025

ABSTRACT: Liquefaction evaluation can use deterministic or probabilistic methods. The deterministic approach is limited by its inability to address uncertainty from soil complexity and heterogeneity, as well as the probabilistic nature of earthquakes. This method is often inadequate for accurate liquefaction analysis, as it does not reflect true field conditions. Conversely, probabilistic analysis allows for uncertainty and establishes a safety factor proportional to the associated risk. This research analyzes at how the influence of fine particles affects the likelihood of liquefaction, using the Lind-Hasofer reliability theory. This theory estimates the any probability of reliability (Ro) by converting the nonlinear limit state function into a linear form around the design point. The reliability of liquefaction (Ro) is determined using factors such as earthquake magnitude (Mw), maximum shaking strength (a_{max}/g), total pressure (σ_v), effective pressure (σ'_v), percentage of fine particles (FC), and SPT blow count (N_{SPT}). Results from 16 drilling locations with different amounts of fine particles and earthquake loads show that cyclic resistance increases with $(N_1)_{60CS}$, but decreases when fines content exceeds 35% or when $(N_1)_{60CS} < 13$. The empirical relationship between SF and Ro ($y = 8.898x^{3.0536}$, $R2 > 0.9267$) highlights that some layers with SF ≥ 1 still correspond to low Ro < 0.8, indicating the limitations of deterministic analysis. Overall, the probabilistic approach provides a more realistic and risk-consistent assessment of liquefaction potential, making it more suitable for risk- and performance-based geotechnical design.

Keywords: Liquefaction, Fine-grained, Fosm lind-hasofer, Cyclic-resistance

1. INTRODUCTION

The geotechnical characteristics of the sand layer in the Sleman region, Special Region of Yogyakarta, Indonesia, show a highly variable fines content, ranging from 0.25% to 85%, with shallow groundwater conditions. This combination increases susceptibility to liquefaction during dynamic loads such as earthquakes and has a high potential to cause significant damage to infrastructure. The evaluation of liquefaction potential is very complex due to the complexity and heterogeneity of soil parameters as well as the uncertainty of seismic loads. The deterministic approach, which is widely used, is unable to represent the uncertainties. Probabilistic analysis, on the other hand, helps measure uncertainty and create safety factors based on risk, making it better for evaluating liquefaction potential in varied soil conditions [1-3].

Previous research has shown that the fine particle content in sand can increase the soil resistance to liquefaction compared to clean sand at the same N_{SPT} value. Liquefaction resistance, or cyclic resistance, increase linearly with the value of $(N_1)_{60CS}$, which is influenced by the fines content and soil density [4]. However, more recent investigations indicate that this relationship is not strictly linear. Soils with fines content exceeding approximately 35% often exhibit nonlinear or even diminishing effects, where excess fines may alter the soil fabric and reduce drainage capacity, leading to lower cyclic resistance than predicted by linear correlations [5-6]. Therefore, the influence of fines content on liquefaction resistance is more complex than earlier simplified assumptions, and both soil fabric and plasticity characteristics must be considered.

Thick layers of sand experience excessive pore pressure increase during an earthquake, causing them to lose their shear strength in undrained conditions; this phenomenon is known as liquefaction [7]. Liquefaction in sand is influenced by factors such as the pore ratio, relative density, and vertical pressure, as explained by Seed [8].

Relative density up to 60%, in the response of saturated sand samples to liquefaction with laboratory liquefaction testing using triaxial shows an increase in stiffness [9]. Earthquake excitation with a certain intensity can cause the ground to lose its bearing capacity, resulting in changes to the soil structure in the form of vertical deformation and/or horizontal displacement [10]. N_{SPT} value of less than 15 blows on submerged sand deposits has a high potential for liquefaction [11].

Cyclic triaxial tests, cyclic simple shear tests, and cyclic torsional shear tests are laboratory techniques used to assess liquefaction potential. In the field, the Standard Penetration Test (SPT), Cone Penetration Test / CPT, measurement of shear wave velocity and Dilatometer test results are used to estimate the soil resistance to liquefaction [12-15].

Assessing liquefaction potential caused by earthquakes and the soil resistance to liquefaction using both field and laboratory techniques, is usually assessed by the shear stress and shear strain[13-17]. Field methods for calculating soil resistance to liquefaction using the SPT test results approach are conducted by Youd and Idriss [18]. The approach to cyclic stress and strain must follow three stages, namely: the approach of cyclic shear stress or strain along the depth due to an earthquake, the approach of cyclic shear strength of the soil, and comparing the shear stress due to the earthquake and the soil resistance.

Deterministic assessment of liquefaction potential based on laboratory or field test results generally uses the safety factor (SF) value. In this approach, SF < 1 indicates that the soil is prone to liquefaction, while SF ≥ 1 is considered safe from liquefaction [4, 19]. However, this deterministic method has limitations because it does not consider the spatial variability in the field, such as soil heterogeneity, fluctuations in groundwater levels, and earthquake characteristics. As a result, the reliability of safety assessments based on SF ≥ 1 needs to be re-evaluated. The probabilistic method can provide a more realistic assessment by considering the variability of field conditions. Thus, the probabilistic approach can depict the likelihood of liquefaction occurring, even under conditions where SF ≥ 1.

This study evaluates the influence of fines fractions on sand layers using a probabilistic approach to determine the reliability level of soil structures against liquefaction. The reliability levels obtained from the probabilistic approach will be compared with the deterministic approach. Also, identification of the trend of cyclic resistance in relation to fines content will be discussed in the following. Data was collected at 6 locations with 16 drilling points in Sleman, Special Region of Yogyakarta, which contained fine grain content varying between 0.25% to 85% and analyzed for earthquake strengths ranging from 5 SR to 8 SR, corresponding to earthquakes that have occurred in the Special Region of Yogyakarta. The novelty of this study lies in establishing a direct correlation between the deterministic safety factor (SF) and the probabilistic reliability index (Ro). Unlike previous studies, this approach quantifies cases where layers with SF ≥ 1 still exhibit low reliability (Ro < 0.8), leading to an empirical relationship that provides new insight into the limitations of deterministic analysis and the added value of reliability-based assessment.

2. RESEARCH SIGNIFICANCE

This research offers originality by applying the Lind-Hasofer reliability theory to liquefaction analysis, emphasizing the role of fine particle content in probabilistic evaluation. Unlike conventional deterministic methods, which overlook soil variability and seismic uncertainty, this study integrates fines content (FC) with key seismic and geotechnical parameters to quantify reliability (Ro). The novel empirical correlation between safety factor (SF) and reliability (Ro) demonstrates that layers with SF ≥ 1 may still show low reliability, revealing critical limitations of deterministic approaches. This work advances a more realistic, risk-consistent framework for liquefaction assessment, contributing to performance-based geotechnical design.

3. METHODOLOGY

Using data from 16 borehole points, the fine grain content varies at 5%, 15%, 20%, 35%, 45%, and 5 variations of earthquake strength, namely: 5 SR, 6.8 SR, 7.2 SR, 7.5 SR, and 8 SR, which will be used in the analysis. The methodology in this research is explained as follows.

3.1 Deterministic Approach

The deterministic liquefaction potential evaluation method, developed by Idriss and Boulanger [20] and Hu, et. al [21], is as follows:

3.1.1 Determining Cyclic Stress

Cyclic stress ratio (CSR) can be calculated using Eq. (1). Where a_{max} is peak ground acceleration (in g that is 9.81 m/s²), σ_v and σ'_v are the total and effective vertical stresses, respectively (in kPa), Pa is atmospheric pressure (100 kPa), MSF, r_d and K_σ are the magnitude scaling factor, the depth reduction factor and the overburden correction factor (dimensionless). This correlation is proposed by Seed [8] and subsequently modified in liquefaction evaluation procedures by Youd and Idriss [18].

$$\mathrm{CSR} = \frac{0.65.\frac{\mathbf{a}_{\mathrm{maks}}}{\mathbf{g}}.\sigma_{\mathbf{v}}.r_{\mathbf{d}}}{\sigma o'}.\frac{\mathbf{1}}{\mathrm{MSF}}.\frac{\mathbf{1}}{\mathbf{K}_{\boldsymbol{\sigma}}} \quad (1)$$

3.1.2 Determining Cyclic Resistance

Determining cyclic resistance is conducted by correcting $(N_1)_{60}$ to the standard penetration of clean sand $(N_1)_{60CS}$, after analyzing the fines content (FC) [21]. *Cyclic* Resistance for sandy soil with fine fractions is analysed as per Eq. (2) to Eg. (4) below:

$$\text{Cyclic Resistance} = \exp\left\{\frac{\mathbf{(N_1)_{60cs}}}{\mathbf{14.1}} + \left[\frac{\mathbf{(N_1)_{60cs}}}{\mathbf{126}}\right]^{\mathbf{2}} - \left[\frac{\mathbf{(N_1)_{60cs}}}{\mathbf{23.6}}\right]^{\mathbf{3}} + \left[\frac{\mathbf{(N_1)_{60cs}}}{\mathbf{25.4}}\right]^{\mathbf{3}} - \mathbf{2,8}\right\} \quad (2)$$

$$(\mathbf{N_1})_{60\mathrm{CS}} = (\mathbf{N_1})_{60} + \mathbf{\Delta}(\mathbf{N_1})_{60} \quad (3)$$

To ensure numerical stability in the regression model, a small offset term ε = 0.001was introduced to the fines fraction $f = FC/100$. This prevents singularity at zero fines content and does not affect physical interpretation. Accordingly, Equation (4) is reformulated as:

$$\boldsymbol{\Delta}(\mathbf{N_1})_{60} = \mathbf{exp}\left\{\mathbf{1.63} + \frac{\mathbf{0.097}}{\mathbf{f+\varepsilon}} + \left[\frac{\mathbf{0{,}157}}{\mathbf{f+\varepsilon}}\right]^{\mathbf{2}}\right\} \quad (4)$$

where f is fines content expressed in fractional form

3.1.3 Safety Factor

The factor of safety indicates the relationship between the soil's resistance to liquefaction and the pressure exerted due to earthquake. This relationship varies depending on the depth of the soil layer. Therefore, assessments are carried out at specific depth intervals. The calculation of the safety factor at these depths is shown in Equation (5) below.

$$\text{Safety factor } \rightarrow \text{SF} = \frac{\text{CRR}}{\text{CSR}} \geq \mathbf{1} \quad (5)$$

3.2 Probabilistic Approach

Evaluating the probability of system failure in liquefaction, caused by the complexity and heterogeneity of the soil as well as the probabilistic nature of earthquakes, is not sufficient with a deterministic approach alone. Probabilistic analysis, such as the Hasofer-Lind reliability index method, becomes highly relevant to address the problem.

3.2.1 Hasofer-Lind Reliability Index (β_{HL})

The Hasofer-Lind index defines the shortest distance / design point / Most Probable Point, MPP from the origin to the limit state surface in the space of random variables that have been transformed into independent standard normal variables. as shown in (Fig.1),

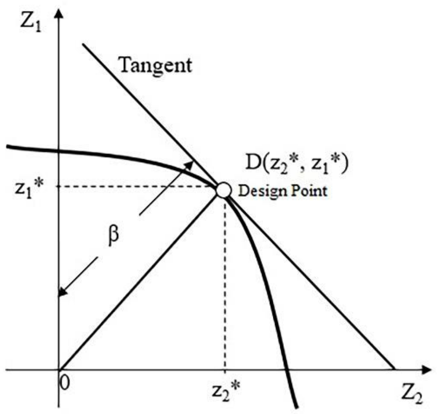

Fig. 1 Hasofer-Lind Reliability Index

The basic formulation is presented by Cornell [22]. A structure with resistance R and receiving a load Q, govern failure surface as explained in Eq. (6) as follows:

$$M = g(R, Q) = R - Q \quad (6)$$

The reduced variable form can be written as Eq. (7), below:

$$\begin{aligned} g(R, Q) &= (\mu_R + Z_R.\ \sigma_R) - (\mu_Q + Z_Q.\ \sigma_Q) \quad (7) \\ &= (\mu_R - \mu_Q) + Z_R.\ \sigma_R - Z_Q.\ \sigma_Q \end{aligned}$$

Therefore, collapse plane equation is described as M = R – Q = 0, which defines the reliability index β, as Eq. (8). μ_M and σ_M are the mean and standard deviation of M.

$$\boldsymbol{\beta} = \frac{\boldsymbol{\mu_M}}{\boldsymbol{\sigma_M}} \quad (8)$$

The concept of the reliability index for the fundamental case (R, Q), are normally distributed through random variables. Safety is defined by the condition M > 0, while failure is defined as M < 0. The reliability index is the closest distance to M = 0. The Cornel equation $\mu_M = \beta\sigma_M$ is also shown in (Fig. 2).

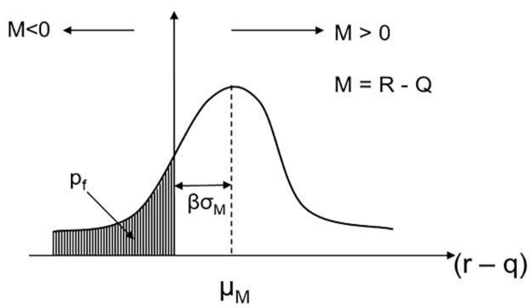

Fig. 2 Reliability Index: R and Q Normal

If R and Q are normal and independent, then using Eq. (9) and Eq. (10),

$$\boldsymbol{\beta} = \frac{\boldsymbol{\mu_R - \mu_Q}}{\sqrt{\boldsymbol{\sigma_R}^2 + \boldsymbol{\sigma_Q}^2}} \quad (9)$$

$$\sqrt{\boldsymbol{\sigma_R}^2 + \boldsymbol{\sigma_Q}^2} = \boldsymbol{\sigma_M} \quad (10)$$

3.2.2 Simultaneous Equation Procedure

Steps to determine the Lind-Hasofer reliability index is explained as follows.
First is to formulate the safety boundary function and the appropriate parameters for the random variables involved. The safety boundary function in Eq. 13 is translated from Eq. 12 incorporating some random variables such as: peak ground acceleration (a_{max}/g) at a location defined as x_1; σ_v total stress defined as x_2; depth factor rd defined as x_3; σ'_v effective stress

defined as x_4; MSF magnitude factor defined as x_5; atmospheric stress factor k_σ defined as x_6; and the clean sand's standard penetration resistance value, $(N_1)_{60CS}$ defined as x_7. Therefore, Eq. (11) and Eq. (12) becomes Eq. (13).

$$G(\,) = CRR - CSR \tag{11}$$

$$\mathbf{g}(\,) = \mathbf{exp}\left\{\frac{(N_1)_{60cs}}{14.1} + \left[\frac{(N_1)_{60cs}}{126}\right]^2 - \left[\frac{(N_1)_{60cs}}{23.6}\right]^3 + \left[\frac{(N_1)_{60cs}}{25.4}\right]^3 - 2,8\right\} - \frac{0.65\,\frac{a_{max}}{g}\,\sigma_v\,r_d}{\sigma'_o}\,\frac{1}{MSF}\,\frac{1}{K_\sigma} \tag{12}$$

$$\mathbf{g}(x_1, x_2, \ldots, x_7) = \mathbf{exp}\left\{\frac{x_7}{14.1} + \left[\frac{x_7}{126}\right]^2 - \left[\frac{x_7}{23.6}\right]^3 + \left[\frac{x_7}{25.4}\right]^3 - 2,8\right\} - \frac{0.65\,x_1\,x_2\,x_3}{x_4}\,\frac{1}{x_5}\,\frac{1}{x_6} \tag{13}$$

The boundary function in terms of the reduced variable Zi, as expressed in Eq. (14), is used to define the relationship between the original variables and their standardized counterparts within the reliability analysis framework.

$$\mathbf{Zi} = \frac{X_i - \mu i}{\sigma_i} \tag{14}$$

When Eq. (12) is equal to zero, by substituting Eq. (14), we obtain the Lind-Hasofer reliability index as shown in Eq. (15) below. This substitution allows us to reformulate the problem in standard form. Next, we express the boundary equations in terms of β and αi, which define the boundary state surfaces in the transformed space. We then obtain the function g(x), which is the performance function for reliability assessment. Through this process, we arrive at Eq. (16) through Eq. (19). These equations allow us to express αi as a function of all values of αi and β, as shown in Eq. (20) through Eq. (22) below.

$$\frac{\delta g}{\delta Z2} = -\frac{\frac{0.65\,X1\,.\,X3}{X5}\,(\sigma 2\,)}{(\sigma 6\;Z_6+\mu 6)(\sigma 4\;Z_4+\mu 4)} \tag{17}$$

$$\frac{\delta g}{\delta Z4} = \frac{\frac{0.65\,X1\,.\,X3}{X5}\,(\sigma 2\;Z_2+\mu 2)}{(\sigma 6\;Z_6+\mu 6)(\sigma 4\;Z_4+\mu 4)^2} \tag{18}$$

$$\frac{\delta g}{\delta Z6} = \frac{\frac{0.65\,X1\,.\,X3}{X5}\,(\sigma 2\;Z_2+\mu 2)}{(\sigma 4\;Z_4+\mu 4)(\sigma 6\;Z_6+\mu 6)^2} \tag{19}$$

$$\beta = \frac{\frac{0.65\,X1\,.\,X3}{X5}\,(\mu 2\,) - \mu 6\sigma 4\left[\exp\left\{\frac{x_7}{14.1}+\left[\frac{x_7}{126}\right]^2-\left[\frac{x_7}{23.6}\right]^3+\left[\frac{x_7}{25.4}\right]^4-2.8\right\}\right]}{\left[\exp\left\{\frac{x_7}{14.1}+\left[\frac{x_7}{126}\right]^2-\left[\frac{x_7}{23.6}\right]^3+\left[\frac{x_7}{25.4}\right]^4-2.8\right\}\right]\left(\sigma 6\,\alpha_6\,\sigma 4\,\beta\alpha_4+\sigma 6\;\alpha_6\,\mu 4+s4\,\alpha_4\,\mu 6-\frac{\frac{0.65\,X1\,.\,X3}{X5}\,(\sigma 2\;\alpha_2)}{\left[\exp\left\{\frac{x_7}{14.1}+\left[\frac{x_7}{126}\right]^2-\left[\frac{x_7}{23.6}\right]^3+\left[\frac{x_7}{25.4}\right]^4-2.8\right\}\right]}\right)} \tag{15}$$

$$g(\,) = \left[\exp\left\{\frac{x_7}{14.1}+\left[\frac{x_7}{126}\right]^2-\left[\frac{x_7}{23.6}\right]^3+\left[\frac{x_7}{25.4}\right]^4-2.8\right\}\right] - \frac{\frac{0.65\,X_1\,.\,X_3}{X_5}\,(\sigma_2\;\beta\alpha_2+\mu_2)}{(\sigma_6\;Z_6+\mu_6)(\sigma_4\;Z_4+\mu_4)} \tag{16}$$

$$\alpha_2 = \frac{-\left[\frac{\frac{0.65\,X1\,.\,X3}{X5}\,(\sigma 2\,)}{(\sigma 6\,\beta\alpha_6\;+\mu 6)(\sigma 4\,\beta\alpha_4\;+\mu 4)}\right]}{\sqrt{\left[\left(\frac{\frac{0.65\,X1\,.\,X3}{X5}\,(\sigma 2\,)}{(\sigma 6\,\beta\alpha_6\,+\mu 6)(\sigma 4\,\beta\alpha_4\;+\mu 4)}\right)^2+\left(\frac{\left[\frac{0.65\,X1\,.\,X3}{X5}\,(\sigma 2\;\beta\alpha_2\,+\mu 2\,)\right]}{(\sigma 4\,\beta\alpha_4+\mu 4)2(\sigma 6\;\beta\alpha_6+\mu 6)}\right)^2+\left(\frac{\left[\frac{0.65\,X1\,.\,X3}{X5}\,(\sigma 2\;\beta\alpha_2\,+\mu 2\,)\right]}{(\sigma 4\,\beta\alpha_4+\mu 4)(\sigma 6\;\beta\alpha_6+\mu 6)2}\right)^2\right]}} \tag{20}$$

$$\alpha_4 = \frac{\left[\frac{\left[\frac{0.65\,X1\,.\,X3}{X5}\,(\sigma 2\;\beta\alpha_2\,+\mu 2\,)\right]}{(\sigma 4\,\beta\alpha_4+\mu 4)2(\sigma 6\;\beta\alpha_6+\mu 6)}\right]}{\sqrt{\left[\left(\frac{\frac{0.65\,X1\,.\,X3}{X5}\,(\sigma 2\,)}{(\sigma 6\,\beta\alpha_6\,+\mu 6)(\sigma 4\,\beta\alpha_4\;+\mu 4)}\right)^2+\left(\frac{\left[\frac{0.65\,X1\,.\,X3}{X5}\,(\sigma 2\;\beta\alpha_2\,+\mu 2\,)\right]}{(\sigma 4\,\beta\alpha_4+\mu 4)2(\sigma 6\;\beta\alpha_6+\mu 6)}\right)^2+\left(\frac{\left[\frac{0.65\,X1\,.\,X3}{X5}\,(\sigma 2\;\beta\alpha_2\,+\mu 2\,)\right]}{(\sigma 4\,\beta\alpha_4+\mu 4)(\sigma 6\;\beta\alpha_6+\mu 6)2}\right)^2\right]}}$$

(21)

$$\alpha_6 = \frac{\left[\frac{\left[\frac{0.65\,X1\,.\,X3}{X5}\;(\sigma 2\;\beta\alpha_2+\mu 2)\right]}{(\sigma 4\;\beta\alpha_4+\mu 4)(\sigma 6\;\beta\alpha_6+\mu 6)2}\right]}{\sqrt{\left[\left(\frac{\frac{0.65\,X1\,.\,X3}{X5}\;(\sigma 2)}{(\sigma 6\;\beta\alpha_6+\mu 6)(\sigma 4\;\beta\alpha_4+\mu 4)}\right)^2+\left(\frac{\left[\frac{0.65\,X1\,.\,X3}{X5}\;(\sigma 2\;\beta\alpha_2+\mu 2)\right]}{(\sigma 4\;\beta\alpha_4+\mu 4)2(\sigma 6\;\beta\alpha_6+\mu 6)}\right)^2+\left(\frac{\left[\frac{0.65\,X1\,.\,X3}{X5}\;(\sigma 2\;\beta\alpha_2+\mu 2)\right]}{(\sigma 4\;\beta\alpha_4+\mu 4)(\sigma 6\;\beta\alpha_6+\mu 6)2}\right)^2\right]}} \tag{22}$$

The process is continued with the first iteration by assuming the values of β and all the values of αi that satisfy Eq. (23). Then the steps that have been explained should be repeated, until the values of β and αi converge.

$$\sum_{i=1}^{n}(\alpha_i)^2 = 1 \tag{23}$$

The iterative solution for β and αi was implemented in MATLAB R2023a using a Newton–Raphson scheme. The algorithm begins with initial guesses of β = 1.0 and αi = 0.5 for each variable. At each step, the partial derivatives (Eqs. 17–19) are evaluated, and the updated β and αi values are computed until the difference between successive iterations satisfies the convergence criterion. This tolerance ensures numerical stability and convergence within fewer than 50 iterations for all cases analyzed.

4. RESULT AND DISCUSSION

Reliability, Ro earthquake strength from 5 SR to 8.0 SR is presented in (Fig. 3). 16 drilling sites at a depth of 30 meters provided the data used in this investigation. The groundwater table height varies from 1 to 12 meters, while the N_{SPT} values range from 3 to 60 blows.

(Fig. 3) shows that with the increase in fines content, the resistance to cyclic resistance increases, and this is observed for all earthquake magnitudes. However, it should be noted that at fines content greater than ±35%, the increase in Ro resistance is no longer significant.

Consequently to (Fig. 3), in (Fig. 4), cyclic resistance increases with the increase in density and fines content. The increase in cyclic resistance of more than ±35% is no longer significant. The observed trend can be explained by microstructural considerations, at moderate fines contents (≈15–35%), fines particles occupy the voids between sand grains, which enhances packing density and reduces the tendency for contractive volumetric strains during cyclic loading. This results in an overall improvement in cyclic strength. However, once the fines content exceeds about 35%, the soil fabric undergoes a transition from a sand-dominated skeleton to a fines-dominated matrix. In this condition, sand particles are dispersed within a continuous fine's framework, which reduces permeability and hampers drainage. The limited dissipation of excess pore water pressure during cyclic loading leads to a faster buildup of pore pressure and consequently a reduction in cyclic strength. This mechanism is consistent with microstructural evidence reported in previous SEM and porosimetry studies by Wei and Yang [23], the threshold fines content practically separates the sand-dominated and fines-dominated structures, with typical values around 30–40%, in line with the interpretation of a mechanical transition

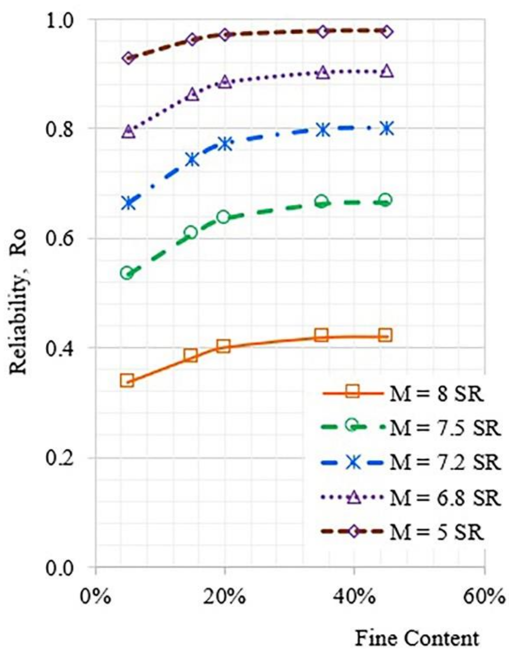

Fig. 3 The relationship between reliability and fines content.

It can be seen in (Fig. 5), cyclic resistance increases with the increase in $(N_1)_{60CS}$, which is directly related to density and fine particle content. The highest and lowest resistances were observed at FC 5% to 45%, respectively. However, the trend reverted once $(N_1)_{60CS}$ hit a value of ±13, with the highest and lowest resistances being 45% and 5%, respectively. To describe the soil's resistance to cyclic movement based on SPT data and fines content, it is crucial to consider the threshold of fine content, which is specified here as $(N_1)_{60CS}$ reaching ±13 (Fig. 5).

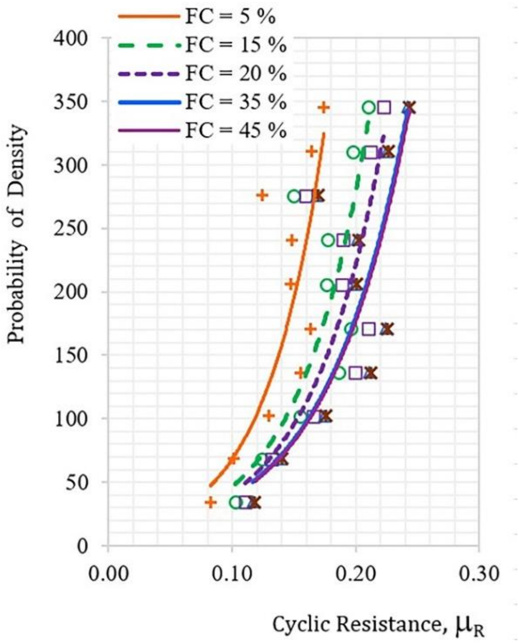

Fig. 4 The relationship between density and cyclic resistance

Furthermore, regression analysis confirms this trend, as the R^2 values for all fines contents are consistently very high ($R^2 = 0.997–1.000$), indicating a strong linear relationship. This statistical evidence justifies the interpretation that cyclic resistance decreases for $(N_1)_{60CS} < 13$, with minor variation observed at low fines content (FC 5%).

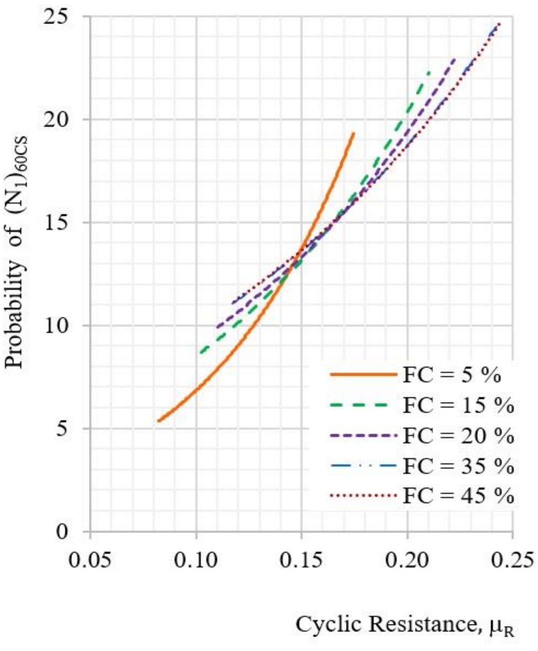

Fig. 5 The relationship between $(N_1)_{60CS}$ and cyclic resistance

In line with the results in (Fig. 3), (Fig. 6) also shows that the resistance to cyclic resistance increases with the increase in $(N_1)_{60CS}$, which is directly related to the density and fine particle content. This is observed for all earthquake magnitudes.

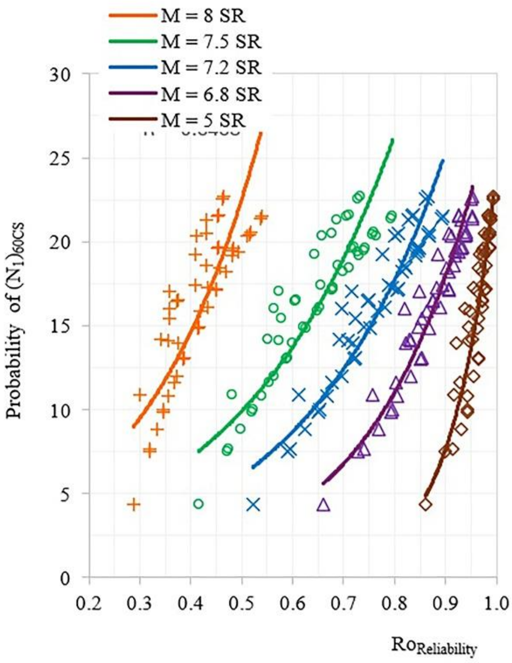

Fig. 6 The relationship between $(N_1)_{60CS}$ and Realibility, Ro

(Fig. 7) presents the relationship between the deterministic Safety Factor (SF) and the Reliability index (Ro) obtained from probabilistic analysis. A positive trend is observed and can be expressed through equation $y = 8.898.x^{3.0536}$. Statistical calculation on (Fig. 7) shows that when $R^2 = 0.927$, the p-values < 0.01, with 95% confidence intervals for both coefficient and exponent. These statistics clarify the uncertainty bounds and support the validity of the proposed correlation within data limitations.

The findings in (Fig.3), (Fig.4), (Fig. 5), and (Fig. 6) are in line with other studies that a small amount of fines in sandy soil can greatly improve cyclic resistance and, thus, results in lower the probability of seismic damage [17-19].

In this study, Mw, a_{max}, and CSR variables were treated as independent to simplify the reliability analysis, following previous liquefaction studies. Although Mw and a_{max} are physically related, site-specific correlations were unavailable; hence independence was assumed. We acknowledge that incorporating correlation structures could further refine the probabilistic model and this will be considered in future work.

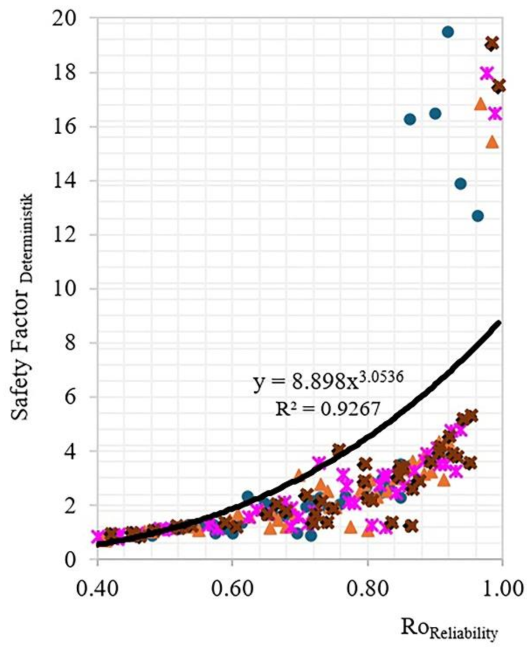

Fig. 7 The relationship between Safety Factor and Reliability, Ro

Practical implication of this study is illustrated in Fig. 8, which presents reliability (Ro) and deterministic safety factor (SF) profiles under varying fines content at an earthquake magnitude of 8 SR. At depths of 6-13m, soils with fines fraction ≥ 35% may appear safe with deterministic SF > 1, yet the probability of liquefaction-induced damage remains about 50%.

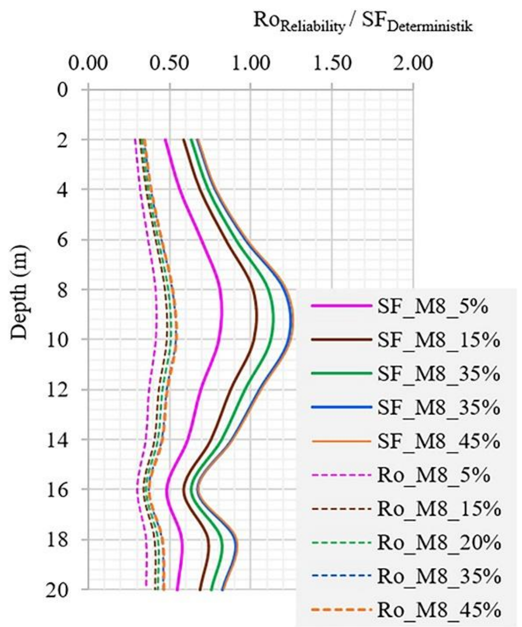

Fig. 8. The relationship depth profiles of Safety Factor and Reliability, Ro

5. CONCLUSION

This research aims to investigate the probability of the influence of fine content expressed as $(N_1)_{60CS}$, cyclic resistance, and soil resistance. The research findings are as follows:

a. Soil resistance to cyclic loading increases with increasing fines content (FC), but this effect is not significant when FC > 35%.
b. Cyclic resistance increases with increasing $(N_1)_{60CS}$, but for $(N_1)_{60CS} < 13$, cyclic resistance decreases with increasing FC.
c. It is found that, although, the deterministic Safety Factor considered as safe (SF ≥ 1), the probabilistic reliability index (Ro) shows a low value (Ro < 0.8).
d. The derived relationship between SF and Ro ($y = 8.898x^{3.0536}$, $R^2 > 0.9267$) confirms the limitations of deterministic methods and the added value of reliability-based evaluation.
e. Cyclic resistance increases with the increase in the value of $(N_1)_{60CS}$, which is directly related to the density and fine particle content.
f. Complementing deterministic analyses with probabilistic approaches may enhance the reliability of liquefaction risk assessment in seismic design.

6. ACKNOWLEDGMENTS

The authors are grateful to the Laboratory of Soil Mechanics, Faculty of Engineering, Atma Jaya University, Yogyakarta, for supporting this study. The authors are also grateful to the Community Service and Research Institute, Atma Jaya Yogyakarta University, for funding allowances provided for education and research.

All parties who have helped collect data and helped carry out this research.

7. REFERENCES

[1] Rahhal M.E., and Zakhem D., Using a reliability-based analysis for evaluating soil liquefaction potential. In 64th Canadian Geotechnical Conference, 14th Pan-American Conference on Soil Mechanics and Geotechnical Engineering, 5th Pan-American Conference on Teaching and Learning of Geotechnical Engineering, 2011.

[2] Kramer S. L., Mayfield R. T., and Huang, Y. M., Performance-based liquefaction potential evaluation. USGS Research Award 06HQGR0041, 2008.

[3] Pratama V., Hardiyatmo H. C., and Saputra, A., Liquefaction potential in waterfront area of Labuan Bajo based on earthquake return period. International Journal of Geomate, Vol. 25, Issue 111, 2023, pp. 104-

112. https://doi.org/10.21660/2023.111.4019
[4] Gunawan S., Hadsari V., Ananda H., and Christina M. N., Fine Content's Impact on Liquefaction-Induced Volumetric Deformation. IOP Conference Series: Earth and Environmental Science, Vol. 1488, No. 1, 2025, pp. 012055. https://doi.org/10.1088/1755.1315/1488/1/012055
[5] Artati H., Pawirodikromo W., Rahardjo P., and Makrup L., Effect of Fines Content on Liquefaction Resistance During Steady-State Conditions. International Journal of Geomate, Vol. 25, Issue 109, 2023, pp. 18-28. https://doi.org/10.21660/2023.109.3481
[6] Wen Liu., and Kamao S., Effect of fines content on liquefaction characteristics. International Journal of Geomate, Vol. 20, Issue 82, 2021, pp. 40-45. https://doi.org/10.21660/2021.82.Gx277
[7] Committee on Soil Dynamics of the Geotechnical Engineering Division, Definition of terms related to liquefaction, Journal of the Geotechnical engineering division,104(9),1978, pp. 1197-1200. https://doi.org/10.1061/ajgeb6.0000688
[8] Seed H. B., Soil liquefaction and cyclic mobility evaluation for level ground during earthquakes, Journal of the geotechnical engineering division, 105(2), 1979, pp. 201-255.
[9] Vaid Y. P., and Thomas J., Liquefaction and postliquefaction behavior of sand, Journal of Geotechnical Engineering, 121(2), 1995, pp. 163-173.
[10] Dashti S., Bray J. D., Pestana J. M., Riemer, M., and Wilson, D., Mechanisms of seismically induced settlement of buildings with shallow foundations on liquefiable soil, Journal of geotechnical and geoenvironmental engineering, 136(1), 2010, pp. 151-164.
[11] Koizumi Y. Changes in density of sand subsoil caused by the Niigata earthquake, Soils and Foundations, 6(2), 1966, pp. 38-44. https://doi.org/10.3208/sandf1960.6.2_38.
[12] Koizumi Y., Changes in density of sand subsoil caused by the Niigata earthquake, Soils and Foundations, 6(2), 1966, pp. 38-44.
[13] Robertson P. K., Liquefaction potential of sands using the cone penetration test, Journal of Geotechnical Division, 22(3), 1985, pp. 298-307. https://doi.org/10.1061/(ASCE)0733-410(1985)111
[14] Andrus R. D., and Stokoe II K. H., Liquefaction resistance of soils from shear-wave velocity, Journal of geotechnical and geoenvironmental engineering, 126(11), 2000, pp. 1015-1025.
[15] Marchetti S., Detection of liquefiable sand layers by means of quasi-static penetration tests, Proc. 2nd European Symp. on Penetration Testing, 1982, pp. 689-695)..
[16] Seed H. B., and Idriss I. M., Simplified procedure for evaluating soil liquefaction potential, Journal of the Soil Mechanics and Foundations division, 97(9), 1971, pp. 1249-1273.
[17] Dobry R., Powell D. J., Yokel F. Y., and Ladd R. S., Liquefaction potential of saturated sand-the stiffness method, In 7th World Conference on Earthquake Engineering Vol. 3, 1980, pp. 25-32.
[18] Youd T. L., and Idriss I. M., Liquefaction resistance of soils: summary report from the 1996 NCEER and 1998 NCEER/NSF workshops on evaluation of liquefaction resistance of soils, Journal of geotechnical and geoenvironmental engineering, 127(4), 2001, pp. 297-313.
[19] Gunawan S., Wijaya W., Hadsari V., and Ekaputra O., Prediksi Deformasi Volumetrik akibat Likuifaksi di Tepian Sungai Tambakbayan Yogyakarta. Jurnal Konstruksi Teknik Sipil, 1(2), 2024, pp. 174-183.
[20] Idriss I. M., and Boulanger R. W., Soil liquefaction during earthquakes, Earthquake Engineering Research Institute, 2008.
[21] Hu Y. X., Liu S. C., and Dong W., Earthquake engineering, 1996, CRC Press.
[22] Cornell C. A., Bounds on the reliability of structural systems, Journal of the structural Division, 93(1), 1967, pp. 171-200.
[23] Wei X., and Yang J., Characterizing the effects of fines on the liquefaction resistance of silty sands, Soils and Foundations, 59(6), 2019, pp. 1800-1812. https://doi.org/10.1016/j.sandf.2019.08.010